Reliable Modeling and Optimization for Chemical Engineering Applications: Interval Analysis Approach

Youdong Lin, C. Ryan Gwaltney and Mark A. Stadtherr*
Department of Chemical and Biomolecular Engineering, University of Notre Dame, Notre Dame, IN 46556, USA

Abstract. In many applications of interest in chemical engineering it is necessary to deal with nonlinear models of complex physical phenomena, on scales ranging from the macroscopic to the molecular. Frequently these are problems that require solving a nonlinear equation system and/or finding the global optimum of a nonconvex function. Thus, the reliability with which these computations can be done often an important issue. Interval analysis provides tools with which these reliability issues can be addressed, allowing such problems to be solved with complete certainty. This presentation will focus on three types of applications: 1) Parameter estimation in modeling of phase equilibrium, including implications of using locally vs. globally optimal parameters in subsequent computations; 2) Nonlinear dynamics, in particular the location of equilibrium states and bifurcations of equilibria in ecosystem models used to assess the risk associated with the introduction of new chemicals into the environment; 3) Molecular modeling, with focus on transition state analysis of diffusion of a sorbate molecule in a zeolite.

1. Introduction

In many applications of interest in chemical engineering it is necessary to deal with nonlinear models of complex physical phenomena, on scales ranging from the macroscopic to the molecular. Frequently these are problems that require solving a nonlinear equation system and/or finding the global optimum of a nonconvex function. Thus, the reliability with which these computations can be done often an important issue. For example, if there are multiple solutions to the model, have all been located? If there are multiple local optima, has the global solution been found? Interval mathematics can provide the modeler with the tools needed to resolve these issues with mathematical and computational certainty, thus providing a degree of problem-solving reliability not available when using standard methods.

In recent years, it has been shown that strategies based on an interval-Newton approach can be used to reliably solve a wide variety of global optimization and nonlinear equation solving problems in chemical engineering, including computation of fluid phase equilibrium from activity coefficient models [35, 42, 45], cubic equation-of state (EOS) models [5, 19, 20, 44] and statistical associating fluid theory [50], calculation of critical points from cubic EOS models [43], location of azeotropes [32] and reactive azeotropes [33], computation of solid-fluid equilibrium [40, 51], parameter estimation using standard least squares [8] and error-in-variables (EIV) [9, 11, 10], and calculation of adsorption in nanoscale pores from a density function theory model [34]. In each case, the interval approach provides a mathematical and computational guarantee either that all solutions have been located in

* Author to whom all correspondence should be addressed. E-mail: markst@nd.edu

a nonlinear equation solving problem or that the global optimum has been found in an optimization problem.

In this paper, we will summarize recent work on three types of applications: 1) Parameter estimation in modeling of phase equilibrium, including implications of using locally vs. globally optimal parameters in subsequent computations; 2) Nonlinear dynamics, in particular the location of equilibrium states and bifurcations of equilibria in ecosystem models used to assess the risk associated with the introduction of new chemicals into the environment; and 3) Molecular modeling, with focus on transition state analysis of diffusion of a sorbate molecule in a zeolite. In the next section, we provide a brief outline of the interval-Newton methodology used for nonlinear equation solving and global optimization in the applications of interest.

2. Background

Several good introductions to interval computations are available [17, 22, 26, 37]. Of particular interest here is the interval-Newton method. Given an $n \times n$ nonlinear equation system $\boldsymbol{f}(\boldsymbol{x}) = \boldsymbol{0}$ with a finite number of real roots in some initial interval, this technique provides the capability to find tight enclosures of *all* the roots of the system that lie within the given initial interval. For the unconstrained minimization of $\phi(\boldsymbol{x})$, a common approach is to seek stationary points, that is, to solve the nonlinear system $\boldsymbol{f}(\boldsymbol{x}) = \boldsymbol{\nabla}\phi(\boldsymbol{x}) = \boldsymbol{0}$. The global optimum will be one of roots of this nonlinear equation system, but there may be other roots as well, representing local optima and saddle points. To identify the global optimum, it is critical that none of the roots be missed, and such a guarantee can be provided by the interval-Newton approach. For a constrained optimization problem, the interval-Newton method can be applied to solve the KKT or Fritz-John conditions. In this section, we first summarize the interval-Newton methodology used, and then give a couple of simple examples that demonstrate the power of the approach.

2.1. Methodology

Given some initial interval $\boldsymbol{X}^{(0)}$, the interval-Newton algorithm is applied to a sequence of subintervals. For a subinterval $\boldsymbol{X}^{(k)}$ in the sequence, the first step is the *function range test*. An *interval extension* $\boldsymbol{F}(\boldsymbol{X}^{(k)})$ of the function $\boldsymbol{f}(\boldsymbol{x})$ is calculated. An interval extension provides upper and lower bounds on the range of values that a function may have in a given interval. It is often computed by substituting the given interval into the function and then evaluating the function using interval arithmetic. Thus the interval extension is often wider than the actual range of function values, but it always includes the actual range. If there is any component of the interval extension $\boldsymbol{F}(\boldsymbol{X}^{(k)})$ that does not include zero, then the interval can be discarded, since no solution of $\boldsymbol{f}(\boldsymbol{x}) = \boldsymbol{0}$ can exist in this interval. The next subinterval in the sequence may then be considered. Otherwise, testing of $\boldsymbol{X}^{(k)}$ continues. During this step, other interval-based techniques (e.g., constraint propagation) may also be applied to try to shrink $\boldsymbol{X}^{(k)}$ before proceeding.

For a global minimization problem, the next step is the *objective range test*. The interval extension $\Phi(\boldsymbol{X}^{(k)})$, containing the range of $\phi(\boldsymbol{x})$ over $\boldsymbol{X}^{(k)}$ is computed. If the lower bound of $\Phi(\boldsymbol{X}^{(k)})$ is greater than a known upper bound on the global minimum, then $\boldsymbol{X}^{(k)}$ can be discarded since it cannot contain the global minimum and need not be further tested. If it is known that $\boldsymbol{X}^{(k)}$ contains a point that can be used to update (reduce) the upper bound on the global minimum (i.e., if the upper bound of $\Phi(\boldsymbol{X}^{(k)})$ is less than the current upper bound on the global minimum), then this update is performed. This can be done in many different ways. A simple, cheap approach that we have used effectively is to evaluate $\phi(\boldsymbol{x})$ at the midpoint of $\boldsymbol{X}^{(k)}$ and use this to update the upper bound. Another approach is to use a local minimization routine starting at the midpoint of $\boldsymbol{X}^{(k)}$. For this purpose, we have used the simple, low-overhead direct search algorithm of Hooke and Jeeves [18, 25]. Use of the local minimizer involves additional computational overhead, but it most cases leads to a better upper bound on the global minimum. In cases when all the stationary points are desired rather than just the global minimum, this test step can be turned off.

The next step is the *interval-Newton test*. The linear interval equation system

$$\boldsymbol{F}'(\boldsymbol{X}^{(k)})(\boldsymbol{N}^{(k)} - \boldsymbol{x}^{(k)}) = -\boldsymbol{f}(\boldsymbol{x}^{(k)}), \tag{1}$$

is solved for a new interval $\boldsymbol{N}^{(k)}$, where $\boldsymbol{F}'(\boldsymbol{X}^{(k)})$ is an interval extension of the Jacobian of $\boldsymbol{f}(\boldsymbol{x})$, and $\boldsymbol{x}^{(k)}$ is an arbitrary point in $\boldsymbol{X}^{(k)}$. It has been shown [17, 26, 37] that any root contained in $\boldsymbol{X}^{(k)}$ is also contained in the *image* $\boldsymbol{N}^{(k)}$. This implies that if the intersection between $\boldsymbol{X}^{(k)}$ and $\boldsymbol{N}^{(k)}$ is empty, then no root exists in $\boldsymbol{X}^{(k)}$, and also suggests the iteration scheme $\boldsymbol{X}^{(k+1)} = \boldsymbol{X}^{(k)} \cap \boldsymbol{N}^{(k)}$. In addition, it has also been shown [17, 26, 37] that, if $\boldsymbol{N}^{(k)} \subset \boldsymbol{X}^{(k)}$, then there is a *unique* root contained in $\boldsymbol{X}^{(k)}$ and thus in $\boldsymbol{N}^{(k)}$. Thus, after computation of $\boldsymbol{N}^{(k)}$ from Eq. (1), there are three possibilities: (1) $\boldsymbol{X}^{(k)} \cap \boldsymbol{N}^{(k)} = \emptyset$, meaning there is no root in the current interval $\boldsymbol{X}^{(k)}$ and it can be discarded; (2) $\boldsymbol{N}^{(k)} \subset \boldsymbol{X}^{(k)}$, meaning that there is *exactly* one root in the current interval $\boldsymbol{X}^{(k)}$; (3) neither of the above, meaning that no conclusion can be drawn. In the last case, if $\boldsymbol{X}^{(k)} \cap \boldsymbol{N}^{(k)}$ is sufficiently smaller than $\boldsymbol{X}^{(k)}$, then the interval-Newton test can be reapplied to the resulting intersection, $\boldsymbol{X}^{(k+1)} = \boldsymbol{X}^{(k)} \cap \boldsymbol{N}^{(k)}$. Otherwise, the intersection $\boldsymbol{X}^{(k)} \cap \boldsymbol{N}^{(k)}$ is bisected, and the resulting two subintervals are added to the sequence (stack) of subintervals to be tested. If an interval containing a unique root has been identified, then this root can be tightly enclosed by continuing the interval-Newton iteration, which will converge quadratically to a desired tolerance (on the enclosure diameter).

This approach is referred to as an interval-Newton/generalized-bisection (IN/GB) method. At termination, when the subintervals in the sequence have all been tested, either all the real roots of $\boldsymbol{f}(\boldsymbol{x}) = \boldsymbol{0}$ have been tightly enclosed, or it is determined that no root exists. Applied to nonlinear equation solving problems, this can be regarded as a type of branch-and-prune scheme on a binary tree. Applied to global optimization problems, with the objective range test turned on, it can be regarded as a type of branch-and-bound scheme, again on a binary tree. It should be emphasized that the enclosure, existence, and uniqueness properties discussed above, which are the basis of the IN/GB method, can be derived without making any strong assumptions about the function $\boldsymbol{f}(\boldsymbol{x})$ for which roots

are sought. The function must have a *finite* number of roots over the search interval of interest; however, no special properties such as convexity or monotonicity are required, and $\boldsymbol{f}(\boldsymbol{x})$ may have transcendental terms.

Clearly, the solution of the linear interval system given by Eq. (1) is essential to this approach. To see the issues involved in solving such a system, consider the general linear interval system $\boldsymbol{A}\boldsymbol{z} = \boldsymbol{B}$, where the matrix $\boldsymbol{A}$ and the right-hand-side vector $\boldsymbol{B}$ are interval-valued. The solution set $\mathbb{S}$ of this system is defined by $\mathbb{S} = \left\{ \boldsymbol{z} \,\middle|\, \tilde{A}\boldsymbol{z} = \boldsymbol{b}, \tilde{A} \in \boldsymbol{A}, \boldsymbol{b} \in \boldsymbol{B} \right\}$. However, in general this set is not an interval and may have a very complex, polygonal geometry. Thus to "solve" the linear interval system, one instead seeks an interval $\boldsymbol{Z}$ containing $\mathbb{S}$. Computing the interval hull (the tightest interval containing $\mathbb{S}$) is NP-hard [39], but there are several methods for determining an interval $\boldsymbol{Z}$ that contains but overestimates $\mathbb{S}$. Various interval-Newton methods differ in how they solve Eq. (1) for $\boldsymbol{N}^{(k)}$ and thus in the tightness with which the solution set is enclosed. By obtaining bounds that are as tight as possible, the overall performance of the interval-Newton approach can be improved, since with a smaller $\boldsymbol{N}^{(k)}$ the volume of $\boldsymbol{X}^{(k)} \cap \boldsymbol{N}^{(k)}$ is reduced, and it is also more likely that either $\boldsymbol{X}^{(k)} \cap \boldsymbol{N}^{(k)} = \emptyset$ or $\boldsymbol{N}^{(k)} \subset \boldsymbol{X}^{(k)}$ will be satisfied. Thus, intervals that may contain solutions of the nonlinear system are more quickly contracted, and intervals that contain no solution or that contain a unique solution may be more quickly identified, all of which leads to a likely reduction in the number of bisections needed.

Frequently, $\boldsymbol{N}^{(k)}$ is computed component-wise using an interval Gauss-Seidel approach, preconditioned with an inverse-midpoint matrix. Though the inverse-midpoint preconditioner is a good general-purpose preconditioner, it is not always the most effective approach [26]. Recently, a hybrid preconditioning approach (HP/RP), which combines a simple pivoting preconditioner with the standard inverse-midpoint scheme, has been described by Gau and Stadtherr [12] and shown to achieve substantially more efficient computational performance than the inverse-midpoint preconditioner alone, in some cases by multiple orders of magnitude. However, it still cannot yield the tightest enclosure of the solution set, which, as noted above, is in general an NP-hard problem. Lin and Stadtherr [29, 31] have recently suggested a strategy (LISS_LP) based on linear programming (LP) for solving the linear interval system, Eq. (1), arising in the context of interval-Newton methods. Using this approach, exact component-wise bounds on the solution set can be calculated, while avoiding exponential time complexity. In numerical experiments [29, 31], LISS_LP has been shown to achieve further computational performance improvements compared with HP/RP.

2.2. Examples

To provide some initial examples of the power of this methodology, we use two global optimization problems, both of which have a very large number of local minima.

2.2.1. *Trefethen Challenge Problem*

This is a global optimization problem given by Trefethen [46] as part of a set of challenge problems in which at least 10 digits of precision were required in the final results. The global

minimum of the function

$$\begin{aligned} f(x,y) = &\exp(\sin(50x)) + \sin(60\exp(y)) + \sin(70\sin(x)) + \sin(\sin(80y)) \\ &- \sin(10(x+y)) + (x^2+y^2)/4 \end{aligned} \tag{2}$$

is sought, where $x \in [-1,1]$ and $y \in [-1,1]$. On the unit square ($[0,1] \times [0,1]$) alone, the function has 667 local minima, as well as many other stationary points.

This global optimization problem was solved successfully, with more than 10 digits of precision, in only 0.16 seconds CPU time on a Sun Blade 1000 model 1600 workstation, using the LISS_LP approach. The results for the global optimum are

$$x \in [-0.02440307969437517, -0.02440307969437516],$$

$$y \in [0.2106124271553557, 0.2106124271553558],$$

and

$$f \in [-3.306868647475245, -3.306868647475232]$$

This proves to be a very easy problem to solve using the interval approach.

2.2.2. *Siirola's Problem*
This problem is to find the global minimum of the function

$$f(\boldsymbol{x}) = 100 \prod_{i=1}^{N} \sum_{j=1}^{5} \left(\frac{j^5}{4425} \cos(j + jx_i) \right) + \frac{1}{N} \sum_{i=1}^{N} (x_i - x_{0,i})^2, \tag{3}$$

where $x_i \in [x_{0,i} - 20, x_{0,i} + 20]$ and $x_{0,i} = 3$, $i = 1, ..., N$. This is used as a test problem by Siirola *et al.* [41]. There are 2048 local minima for the case $N = 2$ and on the order of a hundred million (10^8) local minima for the case $N = 5$. The problem also has multiple (N) global minimizer points. The problems were solved for the cases of $N = 2$ to $N = 6$ on a Dell workstation (1.7 GHz Intel Xeon processor running Linux) using LISS_LP with local minimizer.

Results are shown in Table I. For each value of N, there are N global minimizer points, all of which have been found. The global minimizer points can all be expressed in terms of only two numbers, denoted in Table I as x_i^* and $x_{j\neq i}^*$. The i-th global minimizer point will have the value x_i^* for its i-th element, and the value $x_{j\neq i}^*$ for its other $N-1$ elements. Again this proves to be a relatively easy problem to solve using the interval methodology. The results also show the exponential complexity that may be associated with deterministic global optimization (in general, an NP-hard problem).

The subsequent sections will now focus on three types of actual applications in chemical engineering, involving parameter estimation, nonlinear dynamics, and molecular modeling.

Table I. Global solution of Siirola's problem.

N	Global Minimizer Points x_i^*	$x_{j\neq i}^*$	Global Minimum	CPU time (s)
2	4.6198510288	5.2820519601	-88.1046253312	0.07
3	4.6201099154	5.2824296177	-87.6730486951	2.12
4	4.6202393815	5.2826184940	-87.4572049443	33.95
5	4.6203170683	5.2827318347	-87.3276809494	413.61
6	4.6203688625	5.2828074014	-87.2413242244	4566.42

3. Parameter Estimation in VLE Modeling

Because of its importance in the design of separation systems such as distillation, much attention has been given to modeling the thermodynamics of phase equilibrium in fluid mixtures, especially the case of vapor-liquid equilibrium (VLE). Typically these models take the form of excess Gibbs energy models or equation of state models, with binary parameters in the models determined by parameter estimation from experimental data. As an example, we consider here the estimation from binary VLE data of the energy parameters in the Wilson equation for liquid phase activity coefficient.

3.1. Problem Formulation

Expressed in terms of the molar excess Gibbs energy g^E for a binary system, and the liquid-phase mole fractions x_1 and x_2, the Wilson equation is

$$\frac{g^E}{RT} = -x_1 \ln(x_1 + \Lambda_{12}x_2) - x_2 \ln(x_2 + \Lambda_{21}x_1) \tag{4}$$

from which expressions for the activity coefficients are

$$\ln \gamma_1 = -\ln(x_1 + \Lambda_{12}x_2) + x_2 \left[\frac{\Lambda_{12}}{x_1 + \Lambda_{12}x_2} - \frac{\Lambda_{21}}{\Lambda_{21}x_1 + x_2}\right] \tag{5}$$

$$\ln \gamma_2 = -\ln(x_2 + \Lambda_{21}x_1) - x_1 \left[\frac{\Lambda_{12}}{x_1 + \Lambda_{12}x_2} - \frac{\Lambda_{21}}{\Lambda_{21}x_1 + x_2}\right]. \tag{6}$$

The binary parameters Λ_{12} and Λ_{21} are given by

$$\Lambda_{12} = \frac{v_2}{v_1} \exp\left[-\frac{\theta_1}{RT}\right] \tag{7}$$

$$\Lambda_{21} = \frac{v_1}{v_2} \exp\left[-\frac{\theta_2}{RT}\right], \tag{8}$$

where v_1 and v_2 are the pure component liquid molar volumes, T is the system temperature, R is the gas constant, and θ_1 and θ_2 are the energy parameters that need to be estimated.

Given VLE measurements and assuming an ideal vapor phase, experimental values $\gamma_{1,\text{exp}}$ and $\gamma_{2,\text{exp}}$ of the activity coefficients can be obtained from the relation

$$\gamma_{i,\text{exp}} = \frac{y_{i,\text{exp}} P_{\text{exp}}}{x_{i,\text{exp}} P_i^0}, \quad i = 1, 2, \tag{9}$$

where $x_{i,\text{exp}}$ and $y_{i,\text{exp}}$ are, respectively, the experimental liquid and vapor phase mole fractions of component i, P_{exp} is the experimental pressure, and P_i^0 is the vapor pressure of pure component i at the system temperature T. For the example problem here we follow Gmehling *et al.* [13] and use the relative least squares objective

$$\phi(\boldsymbol{\theta}) \equiv \sum_{j=1}^{n} \sum_{i=1}^{2} \left(\frac{\gamma_{ji,\text{exp}} - \gamma_{ji,\text{calc}}(\boldsymbol{\theta})}{\gamma_{ji,\text{exp}}} \right)^2, \tag{10}$$

where the $\gamma_{ji,\text{calc}}(\boldsymbol{\theta})$ are calculated from the Wilson equation at conditions (temperature, pressure and composition) coincident to those used when measuring $\gamma_{ji,\text{exp}}$, and n is the number of data points.

3.2. Results and Discussion

This parameter estimation problem has been solved for a large number of systems, and results presented in the DECHEMA VLE Data Collection [13]. Gau *et al.* [8] applied an interval-Newton approach to a few systems to determine the globally optimal parameters, and found that, in several cases, the parameters reported in the DECHEMA collection were only locally optimal parameters. A particularly interesting problem is the system benzene(1) – hexafluorobenzene(2), for which there are ten data sets, both isothermal and isobaric, found in DECHEMA. As shown in Table II, using the interval-Newton methodology (IN/GB), new globally optimal parameter values are discovered in five of the ten cases. CPU times are on a Sun Ultra 2/1300 workstation.

While the globally optimal parameter values provide a somewhat better prediction of activity coefficients, as measured by the relative least squares objective ϕ, it is not clear whether this better fit will actually result in more accurate calculations of vapor-liquid equilibrium from the activity coefficient model. To test this, for the five cases in which new globally optimal parameters were found, we used both the locally optimal parameters (DECHEMA) and the globally optimal parameters (IN/GB) to predict the presence and location of homogeneous azeotropes. A homogeneous azeotrope is an equilibrium state in which the vapor and liquid phases have the same composition. Knowledge of azeotropes is critical in the design of distillation operations. Since separation by distillation is based on the difference in composition between liquid and vapor phases, if there is a homogeneous azeotrope at some composition, it will create a bottleneck beyond which no further separation can occur. The method of Maier *et al.* [32], which employs an interval method and is guaranteed to find all homogeneous azeotropes, or determine with certainty that there are none, was used to do the computation of azeotropes.

Table II. Parameter estimation for benzene(1) – hexafluorobenzene(2) system.

Data Set	Volume: Page[1]	Data points	$T(^oC)$ or P (mmHg)	DECHEMA			IN/GB			No. of Minima	CPU time(s)
				θ_1	θ_2	$\phi(\boldsymbol{\theta})$	θ_1	θ_2	$\phi(\boldsymbol{\theta})$		
1*	7:228	10	T=30	437	-437	0.0382	**-468**	**1314**	**0.0118**	2	19.2
2*	7:229	10	40	405	-405	0.0327	**-459**	**1227**	**0.0079**	2	17.6
3*	7:230	10	50	374	-374	0.0289	**-449**	**1157**	**0.0058**	2	15.8
4*	7:233	11	50	342	-342	0.0428	**-424**	**984**	**0.0089**	2	14.1
5	7:231	10	60	-439	1096	0.0047	-439	1094	0.0047	2	12.4
6	7:232	9	70	-424	1035	0.0032	-425	1036	0.0032	2	10.1
7*	7:234	17	P=300	344	-347	0.0566	**-432**	**993**	**0.0149**	2	22.5
8	7:235	16	500	-405	906	0.0083	-407	912	0.0083	2	18.3
9	7:236	17	760	-407	923	0.0057	-399	908	0.0053	1	17.9
10	7:226	29	760	-333	702	0.0146	-335	705	0.0146	2	26.1

[1]Refers to volume and page numbers in DECHEMA VLE Data Collection [13].
*New globally optimal parameters found.

Results of the azeotrope calculations are shown in Table III, along with experimental data indicating that this system has two homogeneous azeotropes. However, when the locally optimal parameters reported in DECHEMA are used in azeotrope prediction, there are three cases in which no azeotrope is found, and in the remaining two cases only one azeotrope is found. Using the globally optimal parameters found using the interval method, two azeotropes are predicted in all cases. In this case, by finding the globally, as opposed to locally, optimal parameter values, it clearly makes the difference between predicting physical reality or not. If the DECHEMA parameters are used, one would conclude that the Wilson equation is a very poor model. However, when the globally optimal parameters values are used, it appears that the Wilson equation is actually a relatively good model, though a better prediction of the azeotrope compositions would be desirable.

The difference between the use of the globally and locally optimal parameters can also have an effect on many other types of calculations. For example, Ulas *et al.* [48] demonstrate how batch distillation optimal control profiles are affected by using the globally optimal parameter values predicted by IN/GB, versus the locally optimal parameters published in DECHEMA. Since batch distillation is a dynamic process, the uncertainties in model parameters are translated into time-dependent uncertainties. Two different time-dependent relative volatility profiles are obtained using global and local parameter values for the Wilson model. These profiles are statistically analyzed and represented by Ito processes. The batch distillation optimal control problem is then solved for three cases: the stochastic global case (relative volatility is represented by an Ito process, obtained from global parameters), the stochastic local case (relative volatility is represented by an Ito process, obtained from local parameters) and the deterministic case (relative volatility is taken as constant). The results of these case studies show that the stochastic global reflux ratio profile results in the highest product yield and the product purity is significantly closer to the specified purity for optimal control.

In addition to problems involving a simple least squares objective, such as discussed above, the interval methodology can also be applied to parameter estimation problems in which the error-in-variables (EIV) approach is used. For example, Gau and Stadtherr [9, 11, 10], consider EIV parameter estimation problems in the modeling of VLE, reaction kinetics, and heat exchange networks, and solve them using the HP/RP algorithm for the interval-Newton method. When the EIV approach is used, the dimensionality of the optimization problem becomes much larger. The largest problem solved was a heat exchanger network problem with 264 variables [11]. Parameter estimation problems that require solving a nonlinear and nonconvex optimization problem, and for which there is thus the potential for multiple local optima, occur in many areas of engineering and science. This is an area in which use of an interval approach to guarantee global optimality could have a significant impact.

Table III. Azeotrope prediction for benzene(1) – hexafluorobenzene(2) system.

Data	$T(^oC)or$	DECHEMA			IN/GB			Experiment		
Set	P (mmHg)	x_1	x_2	P or T	x_1	x_2	P or T	x_1	x_2	P or T
1	T=30	0.0660	0.9340	P=107	0.0541	0.9459	P=107	0.15	0.85	P=107
					0.9342	0.0658	121	0.95	0.05	120
2	40	0.0315	0.9685	168	0.0761	0.9239	168	0.16	0.84	167
					0.9244	0.0756	185	0.93	0.07	183
3	50	NONE			0.0988	0.9012	255	0.17	0.83	254
					0.9114	0.0886	275	0.90	0.10	273
4	50	NONE			0.0588	0.9412	256	0.17	0.83	254
					0.9113	0.0887	274	0.90	0.10	273
7	P=300	NONE			0.1612	0.8388	T=54.13	0.20	0.80	T=54.55
					0.9315	0.0685	52.49	0.89	0.11	52.50

4. Nonlinear Dynamics: Ecological Modeling

A problem of frequent interest in many fields of science and engineering is the study of nonlinear dynamics. Through the use of bifurcation diagrams, a large amount of information concerning the number and stability of equilibria in a nonlinear ODE model can be concisely represented. Bifurcations of equilibria are typically found by solving a nonlinear algebraic system consisting of the equilibrium (steady-state) conditions along with one or more augmenting functions. Typically this equation system is solved using some continuation-based tool (e.g., AUTO [6]). However, in general, these methods do not provide any guarantee that all bifurcations will be found, and are often initialization dependent. Thus, without some *a priori* knowledge of system behavior, one may not know with complete certainty if all bifurcation curves have been identified and explored. We demonstrate here the use of an interval-Newton methodology as a way to ensure that *all* equilibrium states and bifurcations of interest are found.

In particular, we are interested in locating equilibrium states and bifurcations in food chain models. These models are descriptive of a wide range of behaviors in the environment, and are useful as a tool to perform ecological risk assessments. Our interest in ecological modeling is motivated by its use as one tool in studying the impact on the environment of the industrial use of newly discovered materials. Clearly it is preferable to take a proactive, rather than reactive, approach when considering the safety and environmental consequences of using new compounds. Of particular interest is the potential use of room temperature ionic liquid (IL) solvents in place of traditional solvents [4]. IL solvents have no measurable vapor pressure and thus, from a safety and environmental viewpoint, have several potential advantages relative to the traditional volatile organic compounds (VOCs) used as solvents, including elimination of hazards due to inhalation, explosion and air pollution. However, ILs are, to varying degrees, soluble in water; thus, if they are used industrially on a large scale, their entry into the environment via aqueous waste streams is of concern. The effects of trace levels of ILs in the environment are today essentially unknown and thus must be studied. Single species toxicity information is very important as a basis for examining the effects that a contaminant will have on an environment. However, this information, when considered by itself, is insufficient to predict impacts on a food chain, food web, or an ecosystem. Ecological modeling provides a means for studying the impact of such perturbations on a localized environment by focusing not just on the impact on one species, but rather on the larger impacts on the food chain and ecosystem. Of course, ecological modeling is just one part of a much larger suite of tools, including toxicological [7, 21], hydrological and microbiological studies, that must be used in addressing this issue.

Food chain models are often simple, but display rich mathematical behavior, with varying numbers and stability of equilibria that depend on the model parameters (e.g., [14, 36]). Therefore, bifurcation analysis is quite useful in characterizing the mathematical behavior of predator/prey systems, as it allows for the concise representation of model behavior over a wide range of parameters. We will focus on one particular food chain model here, namely a tritrophic (prey, predator, superpredator) Rosenzweig-MacArthur model, as described in much more detail by Gwaltney *et al.* [16]

4.1. Problem Formulation

The Rosenzweig-MacArthur model features a logistic prey ($i = 1$), and hyperbolic (Holling Type II) predator ($i = 2$) and superpredator ($i = 3$) responses. In terms of the biomasses x_1, x_2 and x_3, the model is given by

$$\frac{dx_1}{dt} = x_1 \left[r\left(1 - \frac{x_1}{K}\right) - \frac{a_2 x_2}{b_2 + x_1} \right] \tag{11}$$

$$\frac{dx_2}{dt} = x_2 \left[e_2 \frac{a_2 x_1}{b_2 + x_1} - \frac{a_3 x_3}{b_3 + x_2} - d_2 \right] \tag{12}$$

$$\frac{dx_3}{dt} = x_3 \left[e_3 \frac{a_3 x_2}{b_3 + x_2} - d_3 \right]. \tag{13}$$

Here r is the prey growth rate constant, K is the prey carrying capacity of the ecosystem, the d_i are death rate constants, the a_i represent maximum predation rates, the b_i are half-saturation constants, and the e_i are predation efficiencies.

The equilibrium (steady-state) condition is simply

$$d\mathbf{x}/dt = \mathbf{0}, \tag{14}$$

which in this case is subject to the feasibility condition $\mathbf{x} \geq \mathbf{0}$. Thus, once all the model parameters have been specified, there is a 3×3 system of nonlinear equations to be solved for the equilibrium states. The stability of these states can be determined from the eigenvalues of the Jacobian J (of $d\mathbf{x}/dt$). According to linear stability analysis, for an equilibrium state to be stable, all of the eigenvalues of the Jacobian must have negative real parts. In addition to equilibrium states, we are also interested in computing bifurcations of equilibria. These include the appearance and disappearance of equilibrium states (fold or saddle node bifurcation), the exchange of stability of two equilibria (transcritical bifurcation), and the change of stability of an equilibrium point (Hopf bifurcation). Three types of codimension-1 bifurcations, namely fold, transcritical and Hopf, and two types of codimension-2 bifurcations, namely double-fold (or double-zero) and fold-Hopf are of particular interest. For codimension-1 bifurcations there is one free parameter and one additional augmenting condition that must be satisfied. For a fold or transcritical bifurcation the additional condition is that an eigenvalue of the Jacobian is zero, or equivalently

$$\det[J(\mathbf{x}, \alpha)] = 0, \tag{15}$$

where α is the free parameter. For a Hopf bifurcation the additional condition is that the Jacobian has a pair of complex conjugate eigenvalues whose real parts are zero. This condition can also be expressed [28] in terms of a bialternate product as

$$\det[2J(\mathbf{x}, \alpha) \odot I] = 0. \tag{16}$$

It can also be shown that to locate a double-fold or a fold-Hopf codimension-two bifurcation of equilibrium, the equilibrium condition can be augmented with the two additional

equations

$$\det[J(\mathbf{x}, \alpha, \beta)] = 0 \tag{17}$$

$$\det[2J(\mathbf{x}, \alpha, \beta) \odot I] = 0 \tag{18}$$

and two additional variables (free parameters) α and β.

Whether one is looking for equilibrium states, or the bifurcations of equilibria discussed above, there is a system of nonlinear equations to be solved that may have multiple solutions, or no solutions, and the number of solutions may be unknown *a priori*. For simple models, including the Rosenzweig-MacArthur model, it may be possible to solve for some of equilibrium states and bifurcations analytically, but for more complex models a computational method is needed that is capable of finding, with certainty, all the solutions of the nonlinear equation system.

4.2. Results and Discussion

Following Gragnani *et al.* [14], the parameters used were set to $a_2 = 5/3$, $b_2 = 1/3$, $e_2 = 1$, $d_2 = 0.4$, $a_3 = 0.05$, $b_3 = 0.5$, $e_3 = 1$, and $d_3 = 0.01$. A bifurcation diagram with the prey carrying capacity, K, and the prey growth rate constant, r, as the free parameters was then computed using the IN/GB methodology, with the result shown in Fig. 1. In an r vs. K bifurcation diagram the values of r at which bifurcations occur are plotted as a function of K. Such a diagram was generated here by using the IN/GB method to repeatedly solve the augmented systems for r and $\boldsymbol{x}$ for slightly different values of K, going from $K = 0$ to $K = 2$ in steps of $K = 0.005$. There may be some values of K for which one of the augmented systems has an infinite number of solutions for r (i.e., the vertical line in Fig. 1). This case cannot be handled directly by the IN/GB technique, or could be missed entirely by the stepping in K. Thus, to ensure that all of the bifurcations are found, it is necessary to also scan in the r direction. That is, the IN/GB method was also used to repeatedly solve the augmented systems for K and $\boldsymbol{x}$ for slightly different values of r, in this case going from $r = 0$ to $r = 2$ in steps of $r = 0.005$. To locate codimension-two bifurcations (double-fold and fold-Hopf), the IN/GB method was used to solve the doubly-augmented system given by Eqs. (14,17,18) for K, r and $\boldsymbol{x}$. The average CPU time (1.7 GHz Intel Xeon processor running Linux) for each solution of Eqs. (14,15) for fold and transcritical bifurcations was about 0.6 seconds, and for each solution of Eqs. (14,16) for Hopf bifurcations was about 1.4 seconds. Solving Eqs. (14,17,18) for codimension-two bifurcations required about 39 seconds. The initial intervals used for the components of $\boldsymbol{x}$ were in all cases [0, 5000] and for the parameters K and r were [0, 2].

As shown in Fig. 1, fold and transcritical of equilibria curves were both found, and are labeled FE and TE respectively. Hopf bifurcation curves were also found, and are labeled H or H_p (for planar Hopf). A planar Hopf bifurcation is one that occurs in a independent two-variable subset of state space. A single fold-Hopf bifurcation was located; this point is represented as an open diamond and labeled FH (no double-fold bifurcations were found). This bifurcation diagram corresponds exactly with the known K vs. r bifurcation diagram for this model, as reported by Gragnani *et al.* [14] This confirms the utility and accuracy of

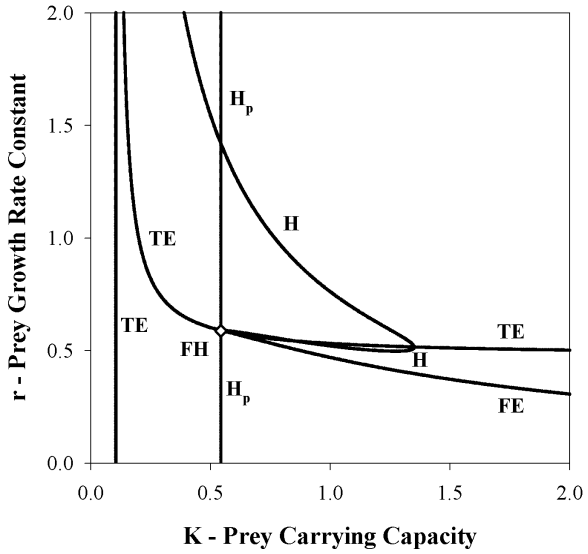

Figure 1. Bifurcation diagram of r vs. K. TE: Transcritical of equilibrium; FE: Fold of equilibrium; H: Hopf; H_p: Planar Hopf; FH: Fold-Hopf codimension-2.

the IN/GB algorithm for computing bifurcation of equilibria diagrams. Bifurcation diagrams such as this can be very easily and automatically generated using the IN/GB methodology, with complete certainty that all bifurcation curves have been found.

Using the same procedure as described above, a d_2 vs. K bifurcation diagram for the Rosenzweig-MacArthur model was also generated. The predator death rate constant d_2 is now a free parameter, and r is now a fixed parameter set at $r = 1$. The resulting bifurcation diagram is shown in Fig. 2. This diagram illustrates that at a constant prey carrying capacity and growth rate constant ($r = 1$), increasing or decreasing the predator death rate will cause macroscopic changes (bifurcations) in system behavior. For relatively small values of K, there are two transcritical bifurcations that occur as d_2 is changed, and for larger values of K there are also two Hopf bifurcations. No double-fold or fold-Hopf codimension-two bifurcations were found. In order to more closely observe these changes in behavior, solution branch diagrams showing the equilibrium states were generated by using IN/GB to solve Eq. (14) for the case of $K = 1$. Fig. 3 gives the solution branch diagrams for $\boldsymbol{x}$ as d_2 is varied from 0 to 2.

Based on the bifurcation diagram (Fig. 2) at $K = 1$, we would expect that as d_2 is increased from 0 to 2, there should be observed first a Hopf bifurcation (the planar Hopf is not observed in this case, due to the sign of the third eigenvalue) and then two transcritical bifurcations. This is what is in fact seen in Fig. 3. These diagrams illustrate that there is a minimum predator death rate constant d_2 that results in stable system behavior. At low predator death rates, the system is unstable and likely exhibits cycles of population booms and busts. As the predator death rate increases, enough predators are dying off at

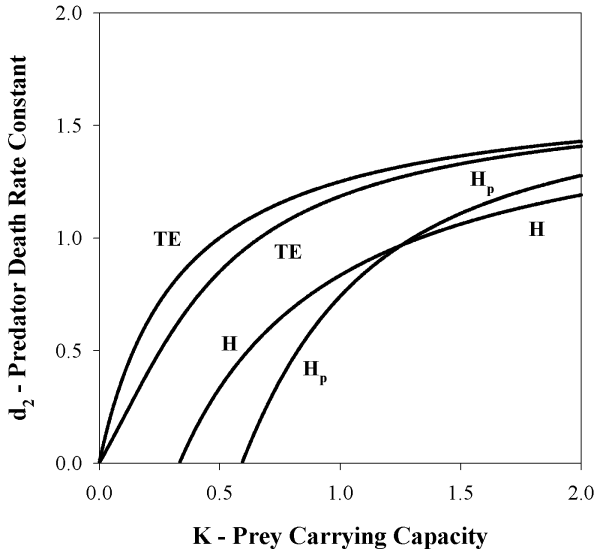

Figure 2. Bifurcation diagram of d_2 vs. K. TE: Transcritical of equilibrium; FE: Fold of equilibrium; H: Hopf; H_p: Planar Hopf.

any given time to prevent the cycles from occurring, and the cycles collapse to a stable steady-state in a Hopf bifurcation. These results also give a sense of the effects of releasing a toxin that specifically targets the predator trophic level, and increases the predator death rate constant. Prior to examining these diagrams, one would expect that such a release would have an impact on both the predator and the superpredator populations. The plot of x_3 in Fig. 3 shows that increasing the predator death rate constant causes a linear decrease in the stable superpredator biomass. However, according to the plot of x_2 in Fig. 3, the stable predator population is not affected until the superpredator population reaches zero. Though these results may seem somewhat counterintuitive, they are indicative of the complex interactions that may occur in food chains. An ecotoxin released at a very low concentration could affect organisms at different trophic levels to varying degrees. For the case considered here, one might observe an impact on the superpredator population and thus assume that the effect of the ecotoxin was at that level, even though the actual effect is on the predator level (death rate constant d_2). Using models such as this one can obtain insights into the impacts of an ecotoxin that might not otherwise be apparent.

The interval methodology has been applied successfully to several other ecological models by Gwaltney *et al.* [16] and Gwaltney and Stadtherr [15]. We anticipate that this methodology will also be useful for computing equilibrium states and bifurcations of equilibria in a wide variety of other problems in engineering and science in which nonlinear dynamical behavior is of interest.

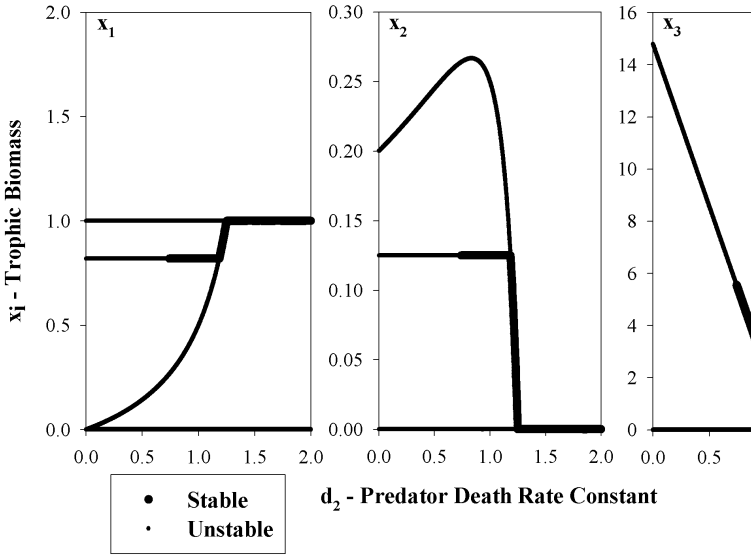

Figure 3. Solution branch diagram illustrating the change in equilibrium states (species biomass) with changes in d_2. From left to right: prey, predator, and superpredator biomasses. $K = 1$ and $r = 1$ for all three plots.

5. Molecular Modeling: Transition State Analysis

Transition-state theory is a well-established methodology which, by providing an approach for computing the kinetics of infrequent events, is useful in the study of numerous physical systems. Classically, it assumes that there exists a potential energy hypersurface which divides the space into a reactant region and a product region. Although the theory was originally for interpretation of chemical reaction rates, it can be amended for non-reacting systems, including desorption/adsorption and diffusion processes in which no chemical bonds are broken or made.

Of particular interest here is the problem of computing the diffusivity of a sorbate molecule in a zeolite. This can be done using the methodology of transition-state theory, as described by June *et al.* [23] It is assumed that diffusive motion of the sorbate molecules through the zeolite occurs by a series of uncorrelated hops between potential minima in the zeolite lattice. A sorption state or site is constructed around each minimum of the potential energy hypersurface. A first order rate constant, k_{ij}, is then associated with the rate of transition between a given pair of neighboring sites, i and j. Any such pair of sites is then assumed to be separated by a dividing surface on which a saddle point of the potential energy hypersurface is located. The saddle point can be viewed as the transition state between sites, and a couple of steepest decent paths from the saddle point connect the minima associated with the i and j sites. After rate constants have been determined for all possible transitions between the sorption sites, a continuous-time/discrete-space Monte Carlo calculation can

then be used to determine the self-diffusivity of the sorbate molecules. Obviously, in this application, and in other applications of transition-state theory, finding all local minima and saddle points of the potential energy surface, $\mathcal{V}$, is critical. We demonstrate here, using a sorbate-zeolite system, the use of the interval-Newton methodology to find all stationary points of a potential energy surface.

Stationary points satisfy the condition $\boldsymbol{g} = \boldsymbol{\nabla}\mathcal{V} = \mathbf{0}$; that is, at a stationary point the gradient of the potential energy surface is zero. Using the eigenvalues of $H = \nabla^2\mathcal{V}$, the Hessian of the potential energy surface, stationary points can be classified into local minima, local maxima, and saddle points (of order determined by the number of negative eigenvalues). There are a number of methods for locating stationary points. A Newton or quasi-Newton method, applied to solve the nonlinear equation system $\boldsymbol{\nabla}\mathcal{V} = \mathbf{0}$, will yield a solution whenever the initial guess is sufficiently close to a stationary point. This method can be used in an exhaustive search, using many different initial guesses, to locate stationary points. The set of initial guesses to use might be determined by the user (intuitively or arbitrarily) or by some type of stochastic multistart approach. Another popular approach is the use of eigenmode-following methods, as done, for example, by Tsai and Jordan [47]. These methods can be regarded as variations of Newton's method. In an eigenmode-following algorithm, the Newton step is modified by shifting some of the eigenvalues of the Hessian (from positive to negative or vice versa). By selection of the shift parameters, one can effectively find the desired type of stationary points, e.g. minima and first-order saddles. There are also a number of other approaches, many involving some stochastic component, for finding stationary points.

In the context of sorbate-zeolite systems, June *et al.* [23] use an approach in which minima and saddle points are located separately. A three step process is employed in an exhaustive search for minima. First, the volume of the search space (one asymmetric unit) is discretized by a grid with a spacing of approximately 0.2Å, and the potential and gradient vector are tabulated on the grid. Second, each cube formed by a set of nearest-neighbor grid nodes is scanned, and the three components of the gradient vector on the eight vertices of the cube checked for changes in sign. Finally, if all three components are found to change sign on two or more vertices of the cube, a BFGS quasi-Newton minimization search algorithm is initiated to locate a local minimum, using the coordinates of the center of the cube as the initial guess. Two different algorithms are tried for determining the location of saddle points. One searches for global minimizers in the function $\boldsymbol{g}^{\mathrm{T}}\boldsymbol{g}$, i.e. the sum of the squares of the components of the gradient vector. The other algorithm, due to Baker [3], searches for saddle points directly from an initial point by maximizing the potential energy along the eigenvector direction associated with the smallest eigenvalue and by minimizing along directions associated with all other eigenvalues of the Hessian.

All the methods discussed above, however, have a major shortcoming, namely that they provide no guarantee that *all* local minima and first order saddle points will actually be found. One approach to resolving this difficulty is given by Westerberg and Floudas [49], who transform the equation-solving problem $\boldsymbol{\nabla}\mathcal{V} = \mathbf{0}$ into an equivalent optimization problem that has global minimizers corresponding to the solutions of the equation system (i.e., the stationary points of $\mathcal{V}$). A deterministic global optimization algorithm, based on a

branch-and-bound strategy with convex underestimators, is then used to find these global minimizers. Whether or not all stationary points are actually found depends on proper choice of a parameter (alpha) used in obtaining the convex underestimators, and Westerberg and Floudas do not use a method that guarantees a proper choice. However, there do exist techniques [1, 2], based on an interval representation of the Hessian, that in principle could be used to guarantee a proper value of alpha, though likely at considerable expense computationally. We demonstrate here an approach in which interval analysis is applied directly to the solution of $\boldsymbol{\nabla}\mathcal{V} = \mathbf{0}$ using an interval-Newton methodology. This provides a mathematical and computational *guarantee* that *all* stationary points of the potential energy surface will be found (or, more precisely, enclosed within an arbitrarily small interval).

5.1. Problem Formulation

Zeolites are materials in which AlO_4 and SiO_4 tetrahedra are the building blocks of a variety of complex porous structures characterized by interconnected cavities and channels of molecular dimensions [24]. Silicalite contains no aluminum and thus no cations; this has made it a common and convenient choice as a model zeolite system. The crystal structure of silicalite, well known from X-ray diffraction studies [38], forms a three-dimensional interconnected pore network through which a sorbate molecule can diffuse. In this work, the phase with orthorhombic symmetry is considered and a rigid lattice model, in which all silicon and oxygen atoms in the zeolite framework are occupying fixed positions and there is perfect crystallinity, is assumed. One spherical sorbate molecule (united atom) will be placed in the lattice, corresponding to infinitely dilute diffusion. The system is comprised of 27 unit cells, each of which is $20.07 \times 19.92 \times 13.42$Å with 96 silicon atoms and 192 oxygen atoms.

All interactions between the sorbate and the oxygen atoms of the lattice are treated atomistically with a truncated Lennard-Jones 6-12 potential. That is, for the interaction between the sorbate and oxygen atom i the potential is given by

$$\mathcal{V}_i = \begin{cases} \frac{a}{r_i^{12}} - \frac{b}{r_i^6} & r_i < r_{\text{cut}} \\ 0 & r_i \geq r_{\text{cut}}, \end{cases} \tag{19}$$

where a is a repulsion parameter, b is an attraction parameter, r_{cut} is the cutoff distance, and r_i is the distance between the sorbate and oxygen atom i. This distance is given by

$$r_i^2 = (x - x_i)^2 + (y - y_i)^2 + (z - z_i)^2, \tag{20}$$

where (x, y, z) are the Cartesian coordinates of the sorbate, and $(x_i, y_i, z_i), i = 1, \ldots, N$ are the Cartesian coordinates of the N oxygen atoms. The silicon atoms, being recessed within the SiO_4 tetrahedra, are neglected in the potential function [27]. Therefore, the total potential energy, $\mathcal{V}$, of a single sorbate molecule in the absence of neighboring sorbate molecules is represented by a sum over all lattice oxygens,

$$\mathcal{V} = \sum_{i=1}^{N} \mathcal{V}_i. \tag{21}$$

The interval-Newton methodology will be applied to determine the sorbate locations (x, y, z) that are stationary points on the potential energy surface $\mathcal{V}$ given by Eq. (21), that is, to solve the nonlinear equation system $\boldsymbol{\nabla}\mathcal{V} = \mathbf{0}$. To achieve tighter interval extensions of the potential function and its derivatives, and thus improve the performance of the interval-Newton method, the mathematical properties of the Lennard-Jones potential and its first- and second-order derivatives can be exploited, as described in detail by Lin and Stadtherr [30].

5.2. Results and Discussion

The interval-Newton methodology described above (LISS_LP) is now applied to find the stationary points of the potential energy surface $\mathcal{V}$ for the case of xenon as a sorbate in silicalite, as described by June *et al.* [23] Due to the orthorhombic symmetry of the silicalite lattice, the search space is only one asymmetric unit, $[0, 10.035] \times [0, 4.98] \times [0, 13.42]$Å, which is one-eighth of a unit cell. This defines the initial interval for the interval-Newton method, namely $X^{(0)} = [0, 10.035]$Å, $Y^{(0)} = [0, 4.98]$Å, and $Z^{(0)} = [0, 13.42]$Å. Following June *et al.* [23], stationary points with extremely high potential, such as $\mathcal{V} > 0$, will not be sought. To do this, we calculate the interval extension of $\mathcal{V}$ over the interval currently being tested, and if its lower bound is greater than zero, then the current interval is discarded. All computations were performed on a Dell workstation running a 1.7 GHz Intel Xeon processor under Linux.

Using the LISS_LP strategy for the interval-Newton method, a total of 15 stationary points were found in a computation time of 724 s. The locations of the stationary points, their energy value, and their type are listed in Table IV. Five local minima were found, along with 8 first-order saddle points and two second-order saddle points. June *et al.* [23] report the same five local minima, as well as 9 of the 10 saddle points. They do not report finding the lower energy second-order saddle point (saddle point #14 in Table IV).

For each first-order saddle point in Table IV, we followed June *et al.*'s method [23] to associate the saddle point with the transition state between two specific minima. The saddle point first was perturbed by 10^{-5}Å in either direction along the eigenvector of the Hessian matrix associated with the negative eigenvalue. A steepest descent method using a step of 0.01Å was taken in the direction $-\boldsymbol{g}$. After 500 iterations, the steepest descent calculation was terminated and a Newton method was used to locate the minima connected through the saddle point. The results of these calculations are given in the rightmost column of Table IV. For example, the lowest energy saddle point (#6) can be viewed as connecting minima #1 and #3. In some cases the descent path from a saddle point led to a state outside the initial search box. Since the search box is one asymmetric unit, for each state found outside the search box, we can always find the equivalent state inside the search box through the symmetry operator and/or the periodic operator. In Table IV this is indicated by marking the state number with a prime. Thus, saddle point #7 connects minimum #2 with an equivalent point in a neighboring asymmetric unit. As expected, the results found for the states connected by the first-order saddle points is consistent with the analysis of June *et al.* [23]

Table IV. Stationary points of the potential energy surface of xenon in silicalite

No.	Type	Energy(kcal/mol)	x(Å)	y(Å)	z(Å)	Connects
1	minimum	-5.9560	3.9956	4.9800	12.1340	
2	minimum	-5.8763	0.3613	0.9260	6.1112	
3	minimum	-5.8422	5.8529	4.9800	10.8790	
4	minimum	-5.7455	1.4356	4.9800	11.5540	
5	minimum	-5.1109	0.4642	4.9800	6.0635	
6	1st order	-5.7738	5.0486	4.9800	11.3210	(1, 3)
7	1st order	-5.6955	0.0000	0.0000	6.7100	(2′, 2)
8	1st order	-5.6060	2.3433	4.9800	11.4980	(1, 4)
9	1st order	-4.7494	0.1454	3.7957	6.4452	(2, 5)
10	1st order	-4.3057	9.2165	4.9800	11.0110	(3, 4)
11	1st order	-4.2380	0.0477	3.9147	8.3865	(2, 4)
12	1st order	-4.2261	8.6361	4.9800	12.8560	(3, 5′)
13	1st order	-4.1405	0.5925	4.9800	8.0122	(4, 5)
14	2nd order	-4.1404	0.5883	4.8777	8.0138	(4,5),(4,4′)
15	2nd order	-4.1027	9.1881	4.1629	11.8720	(2,3),(4,5)

A similar procedure was used on the two second-order saddle points, but using both negative eigenvalues. For example, in the case of saddle point #15, beginning with perturbations in either direction along the eigenvector associated with the most negative eigenvalue leads to a connection between minima #2 and #3. Repeating with the least negative eigenvalue leads to a connection between minima #4 and #5. Thus, this saddle point can be viewed as providing a crossconnection involving these four points. However, there are lower energy connections between all except #2 and #3. Though June *et al.* [23] do not identify this point as a second-order saddle, they do identify it as associating minima #2 and #3.

The second-order saddle point #14, not reported by June *et al.* [23], is very close to the first-order saddle point #13, and slightly lower in energy. Apparently neither of the two methods tried by June *et al.* [23] was able to locate this point. The first method they tried uses the same grid-based optimization scheme used to locate local minima in $\mathcal{V}$, but instead applied to minimize $\boldsymbol{g}^{\mathrm{T}}\boldsymbol{g}$. However, stationary points #13 and #14 are approximately 0.1Å apart, while the grid spacing they used was approximately 0.2Å. This illustrates the danger in using grid-based schemes for finding all solutions to a problem. By using the interval methodology described here, one never needs to be concerned about whether or not a grid spacing is fine enough to find all solutions. The second method they tried was Baker's algorithm [3], as described briefly above, but it is unclear how they initialized the algorithm. A key advantage of the interval method is that no point initialization is required. Only an initial *interval* must be supplied, here corresponding to one asymmetric unit, and this

is determined by the geometry of the zeolite lattice. Thus, in this context the interval methodology is initialization independent.

Lin and Stadtherr [30] have also studied two other sorbate-zeolite systems, and used the interval methodology to find all stationary points on the potential energy surfaces. While we have concentrated here on problems involving transition-state analysis of diffusion in zeolites, we anticipate that the methodology will be useful in many other types of problems in which transition-state theory is applied.

6. Concluding Remarks

We have demonstrated that the interval-Newton approach is a powerful, deterministic approach to the solution of a number of global optimization problems, as well as nonlinear equation solving problems, such as those that arise in chemical engineering and other areas of engineering and science. Problems with a very large number of local optima can be effectively solved, as can problems with a relatively large number of variables. Continuing improvements in methodology, together with advances in software and hardware will make this an increasingly attractive problem solving tool.

The validation provided by the interval approach comes at the expense of additional computation time. Essentially one has a choice between fast methods that may give the wrong answer, or a slower method that is guaranteed to give the correct answer. Thus, a modeler may need to consider the trade off between the additional computing time and the risk of getting the wrong answer to a problem. Certainly, for "mission critical" situations, the additional computing expense is well spent.

Acknowledgements

This work has been supported in part by the National Science Foundation Grant EEC97-00537-CRCD, the Environmental Protection Agency Grant R826-734-01-0, the donors of The Petroleum Research Fund, administered by the ACS, under Grant 35979-AC9, and by the Indiana 21st Century Research & Technology Fund.

References

1. Adjiman, C. S., I. P. Androulakis, and C. A. Floudas: 1998a, 'A Global Optimization Method, Alpha-BB, for General Twice-Differentiable Constrained NLPs – II. Implementation and Computational Results'. *Comput. Chem. Eng.* **22**, 1159.
2. Adjiman, C. S., S. Dallwig, C. A. Floudas, and A. Neumaier: 1998b, 'A Global Optimization Method, Alpha-BB, for General Twice-Differentiable Constrained NLPs – I. Theoretical Advances'. *Comput. Chem. Eng.* **22**, 1137.
3. Baker, J.: 1986, 'An Algorithm for The Location of Transition-States'. *J. Comput. Chem.* **7**, 385–395.

4. Brennecke, J. F. and E. J. Maginn: 2001, 'Ionic Liquids: Innovative Fluids for Chemical Processing'. *AIChE J.* **47**, 2384–2389.
5. Burgos-Solórzano, G. I., J. F. Brennecke, and M. A. Stadtherr: 2004, 'Validated Computing Approach for High-Pressure Chemical and Multiphase Equilibrium'. *Fluid Phase Equilib.* **219**, 245–255.
6. Doedel, E. J., A. R. Champneys, T. F. Fairgrieve, Y. A. Kuznetsov, B. Sandstede, and X. J. Wang: 1997, 'AUTO97: Continuation and Bifurcation Software for Ordinary Differential Equations'. Technical report, Department of Computer Science, Concordia Univeristy, Montreal, Canada.
7. Freemantle, M.: 2002, 'Meeting Briefs: Ionic Liquids Separated From Mixtures by CO_2'. *Chem. Eng. News* **80**(36), 44–45.
8. Gau, C.-Y., J. F. Brennecke, and M. A. Stadtherr: 2000, 'Reliable Parameter Estimation in VLE Modeling'. *Fluid Phase Equilib.* **168**, 1–18.
9. Gau, C.-Y. and M. A. Stadtherr: 2000, 'Reliable Nonlinear Parameter Estimation Using Interval Analysis Error-in-Variable Approach'. *Comput. Chem. Eng.* **24**, 631–638.
10. Gau, C.-Y. and M. A. Stadtherr: 2002a, 'Deterministic Global Optimization for Data Reconciliation and Parameter Estimation Using Error-in-Variables Approach'. In: R. Luus (ed.): *Optimization and Optimal Control in Chemical Engineering*. Trivandrum, India: Research Signpost.
11. Gau, C.-Y. and M. A. Stadtherr: 2002b, 'Deterministic Global Optimization for Error-in-Variables Parameter Estimation'. *AIChE J.* **48**, 1191–1197.
12. Gau, C.-Y. and M. A. Stadtherr: 2002c, 'New Interval Methodologies for Reliable Chemical Process Modeling'. *Comput. Chem. Eng.* **26**, 827–840.
13. Gmehling, J., U. Onken, and W. Arlt: 1977–1990, *Vapor-liquid Equilibrium Data Collection, Chemistry Data Series, Vol. I, Parts 1-8*. Frankfurt/Main, Germany: DECHEMA.
14. Gragnani, A., O. De Feo, and S. Rinaldi: 1998, 'Food Chains in the Chemostat: Relationships between Mean Yield and Complex Dynamics'. *B. Math. Biol.* **60**(4), 703–719.
15. Gwaltney, C. R. and M. A. Stadtherr: 2004, 'Reliable Computation of Equilibrium States and Bifurcations in Nonlinear Dynamics'. In: *Proceedings PARA'04 Workshop on State-of-the-art in Scientific Computing*. Lyngby, Denmark.
16. Gwaltney, C. R., M. P. Styczynski, and M. A. Stadtherr: 2004, 'Reliable Computation of Equilibrium States and Bifurcations in Food Chain Models'. *Comput. Chem. Eng.* in press.
17. Hansen, E. R.: 1992, *Global Optimization Using Interval Analysis*. New York: Marcel Dekker.
18. Hooke, R. and T. A. Jeeves: 1961, 'Direct Search Solution of Numerical and Statistical Problems'. *J. Assoc. Comput. Mach.* **8**, 212–229.
19. Hua, J. Z., J. F. Brennecke, and M. A. Stadtherr: 1998a, 'Enhanced Interval Analysis for Phase Stability Cubic Equation of State Models'. *Ind. Eng. Chem. Res.* **37**, 1519.
20. Hua, J. Z., J. F. Brennecke, and M. A. Stadtherr: 1998b, 'Reliable Computation of Phase Stability Using Interval Analysis Cubic Equation of State Models'. *Comput. Chem. Eng.* **22**, 1207.
21. Jastorff, B., R. St ormann, J. Ranke, K. M olter, F. Stock, and B. Oberheitmann: 2003, 'How Hazardous Are Ionic Liquids? Structure-Activity relationships and biological testing as important elements for sustainability evaluation'. *Green Chemistry* **5**, 136–142.
22. Jaulin, L., M. Kieffer, O. Didrit, and É Walter: 2001, *Applied Interval Analysis*. London: Springer-Verlag.
23. June, R. L., A. T. Bell, and D. N. Theodorou: 1991, 'Transition-State Studies of Xenon and SF_6 Diffusion in Silicalite'. *J. Phys. Chem.* **95**, 8866–8878.
24. Karger, J. and D. M. Ruthven: 1992, *Diffusion in Zeolites and Other Microporous Solids*. New York: Wiley.
25. Kaupe, A. F.: 1963, 'Algorithm 178 Direct Search'. *Commun. ACM* **6**, 313.
26. Kearfott, R. B.: 1996, *Rigorous Global Search: Continuous Problems*. Dordrect, The Netherlands: Kluwer Academic Publishers.
27. Kiselev, A. V., A. A. Lopatkin, and A. A. Shulga: 1985, 'Molecular Statistical Calculation of Gas Adsorption by Silicalite'. *Zeolites* **5**, 1508–1516.
28. Kuznetsov, Y. A.: 1998, *Elements of Applied Bifurcation Theory*. New York: Springer-Verlag.

29. Lin, Y. and M. A. Stadtherr: 2004a, 'Advances in Interval Methods for Deterministic Global Optimization in Chemical Engineering'. *J. Global Optim.* in press.
30. Lin, Y. and M. A. Stadtherr: 2004b, 'Locating Stationary Points of Sorbate-Zeolite Potential Energy Surfaces Using Interval Analysis'. *J. Chem. Phys.* submitted for publication.
31. Lin, Y. and M. A. Stadtherr: 2004c, 'LP Strategy for Interval-Newton Method in Deterministic Global Optimization'. *Ind. Eng. Chem. Res.* **43**, 3741–3749.
32. Maier, R. W., J. F. Brennecke, and M. A. Stadtherr: 1998, 'Reliable Computation of Homogeneous Azeotropes'. *AIChE J.* **44**, 1745.
33. Maier, R. W., J. F. Brennecke, and M. A. Stadtherr: 2000, 'Reliable Computation of Reactive Azeotropes'. *Comput. Chem. Eng.* **24**, 1851–1858.
34. Maier, R. W. and M. A. Stadtherr: 2001, 'Reliable Density-Functional-Theory Calculations of Adsorption in Nanoporous Materials'. *AIChE J.* **47**, 1874–1884.
35. McKinnon, K. I. M., C. G. Millar, and M. Mongeau: 1996, 'Global Optimization for the Chemical and Phase Equilibrium Problem Using Interval Analysis'. In: C. A. Floudas and P. M. Pardalos (eds.): *State of the Art in Global Optimization Computational Methods and Applications*. Dordrecht, The Netherlands: Kluwer Academic Publishers.
36. Moghadas, S. M. and A. B. Gumel: 2003, 'Dynamical and Numerical Analysis of a Generalized Food-chain Model'. *Appl. Math. Comput.* **142**(1), 35–49.
37. Neumaier, A.: 1990, *Interval Methods for Systems of Equations*. Cambridge, England: Cambridge University Press.
38. Olson, D. H., G. T. Kokotailo, S. L. Lawton, and W. M. Meier: 1981, 'Crystal Structure and Structure-Related Properties of ZSM-5'. *J. Phys. Chem.* **85**, 2238–2243.
39. Rohn, J. and V. Kreinovich: 1995, 'Computing Exact Componentwise Bounds on Solution of Linear Systems with Interval Data Is NP-Hard'. *SIAM J. Matrix. Anal.* **16**, 415–420.
40. Scurto, A. M., G. Xu, J. F. Brennecke, and M. A. Stadtherr: 2003, 'Phase Behavior and Reliable Computation of High-Pressure Solid-Fluid Equilibrium with Cosolvents'. *Ind. Eng. Chem. Res.* **42**, 6464–6475.
41. Siirola, J. D., S. Hauen, and A. W. Westerberg: 2002, 'Agent-based Strategies for Multiobjective Optimization'. AIChE Annual Meeting, Indianapolis, IN, Paper 265g.
42. Stadtherr, M. A., C. A. Schnepper, and J. F. Brennecke: 1995, 'Robust Phase Stability Analysis Using Interval Methods'. *AIChE Symp. Ser.* **91**(304), 356.
43. Stradi, B. A., J. F. Brennecke, J. P. Kohn, and M. A. Stadtherr: 2001, 'Reliable Computation of Mixture Critical Points'. *AIChE J.* **47**, 212–221.
44. Stradi, B. A., G. Xu, J. F. Brennecke, and M. A. Stadtherr: 2000, 'Modeling and Design of an Environmentally Benign Reaction Process'. *AIChE Symp. Ser.* **96**(323), 371–375.
45. Tessier, S. R., J. F. Brennecke, and M. A. Stadtherr: 2000, 'Reliable Phase Stability Analysis for Excess Gibbs Energy Models'. *Chem. Eng. Sci.* **55**, 1785.
46. Trefethen, N.: 2002, 'A Hundred-dollar Hundred-digit Challenge'. *SIAM News* **35**, 1.
47. Tsai, C. J. and K. D. Jordan: 1993, 'Use of An Eigenmode Method to Locate The Stationary-Points on The Potential-Energy Surfaces of Selected Argon And Water Clusters'. *J. Phys. Chem.* **97**, 11227–11237.
48. Ulas, S., U. M. Diwekar, and M. A. Stadtherr: 2004, 'Uncertainties in Parameter Estimation and Optimal Control in Batch Distillation'. *Comput. Chem. Eng.* submitted for publication.
49. Westerberg, K. M. and C. A. Floudas: 1999, 'Locating All Transition States and Studying the Reaction Pathways of Potential Energy Surfaces'. *J. Chem. Phys.* **110**, 9259–9295.
50. Xu, G., J. F. Brennecke, and M. A. Stadtherr: 2002, 'Reliable Computation of Phase Stability and Equilibrium from the SAFT Equation of State'. *Ind. Eng. Chem. Res.* **41**, 938–952.
51. Xu, G., A. M. Scurto, M. Castier, J. F. Brennecke, and M. A. Stadtherr: 2000, 'Reliable Computation of High Pressure Solid-Fluid Equilibrium'. *Ind. Eng. Chem. Res.* **39**, 1624–1636.